T. & A. M. REPORT NO. 373

FATIGUE CRACK PROPAGATION IN AN EPOXY POLYMER

BY

STEPHEN A. SUTTON

Contract No. N00019-73-C-0154

Department of the Navy
Naval Air Systems Command

Department of Theoretical and Applied Mechanics

University of Illinois at Urbana-Champaign

June 1973

ABSTRACT

This experimental study investigates the fatigue crack growth rate behavior of an epoxy resin polymer using the tapered-double-cantilever-beam (TDCB) specimen in ambient and elevated temperature environments. An empirical crack growth rate model based on the change in crack extension force, $\Delta \mathcal{G}$, is proposed. Its relation to ΔK models is discussed and observations on the fatigue surface morphology presented.

ACKNOWLEDGMENT

This investigation was conducted in the Department of Theoretical and Applied Mechanics at the University of Illinois. The author wishes to express his appreciation to his advisor, Professor H. T. Corten, for his suggestions, constructive criticism, and encouragement. The assistance of H. T. James and Ruth Ann Stamm in the preparation of the manuscript is gratefully appreciated.

Financial support for the study had been provided by the Department of the Navy, Naval Air System Command, Contract No. N00019-73-C-0154.

TABLE OF CONTENTS

LIST OF SYMBOLS

a	crack length
A	fitted co-efficient in Foreman model; crack area
B	fitted co-efficient in proposed model
b_n	width of fracture surface
C	compliance of TDCB specimen
da/dN	crack growth rate with respect to cycles
E	modulus of elasticity
$\mathcal{G}$	strain energy release rate or crack extension force
$\Delta\mathcal{G}$	change in $\mathcal{G}$ for constant amplitude loading
K	stress intensity factor
ΔK	change in K for constant amplitude loading
K_{max}	maximum K value for constant amplitude loading
K_{min}	minimum K value for constant amplitude loading
K_{mean}	mean K value for constant amplitude loading
m	exponent in proposed fatigue crack growth rate model
n	exponent in models involving ΔK, R
N	cycles
R	stress intensity ratio, K_{min}/K_{max}
γ	geometric shape factor for TDCB specimens
λ	loading parameter in model of ARAD, et al.
δ	crack opening displacement (COD)
σ_y	tensile yield stress
ν	Poisson's ratio

INTRODUCTION

Statement of Problem

From a technological point of view, the adhesive joint has many advantages over the use of conventional fasteners: the alleviation of stress concentrations, the joining of radically dissimilar materials, the ease and economy of fabrication, and, most importantly, the means to fasten the new high-strength, low-weight composites for which metallic fasteners prove unsuitable. Probably the most versatile and widely used bonding agent in high strength applications is the epoxy polymer. In assessing the performance of these epoxies one is led naturally into the broader field of polymers. When epoxies and other polymers are incorporated into service structures, the undermining effects of flaws cause serious strength reductions.

Evidence strongly suggests [1,2]* that in the absence of well-defined slip systems, as found in metals, the process of crack initiation in polymers (especially brittle polymers such as epoxy) is quite different in nature in that the number of cycles needed to initiate a fatigue crack may be quite negligible. That is, polymers are generally endowed with a variety of inhomogeneities and flaws [1,3] which act as stress raisers that may initiate cracks very early in the fatigue life. As a result, the major portion of the fatigue lifetime for these polymers would be spent in fatigue propagation of the cracks. Consequently, quantitative assessment of the crack growth rates is of first order importance. The past two decades have produced an intensive study of the fatigue crack propagation process in metals and a logical step is to extend this analysis into the polymer field.

---

*See List of References at end of report.

This paper explores the behavior of fatigue crack propagation in a relatively pure, well characterized epoxy resin so that the fatgiue strength characteristics of adhesive joints and polymeric materials in general may be better understood and accounted for.

Failure of Adhesive Joints

Failure in adhesive bonds involves principally two types of separations. The interface (IF) separation occurs when the adhesive parts from the adherend. This debonding is typical of stress corrosion failure or weakly bonded systems. The in-the-bond (IB) failure is a separation occurring wholly in the adhesive layer. While the IF separation occurs due to an adhesive failure, the IB separation occurs due to cohesive failure and is thusly governed by the bulk properties of the adhesive subjected to a unique stress state within the adhesive layer. It becomes necessary to examine how these IB cracks behave under cyclic loading in bulk (monolithic) epoxy specimens so that their behavior in complex systems may be predicted using the techniques of fracture mechanics.

FRACTURE MECHANICS BACKGROUND

General

Fracture mechanics attempts to characterize the behavior of flaws, usually sharp cracks, in a body subjected to various applied loads and environments. The two parameters most commonly used to describe the stresses generated at the tip of a sharp crack by an applied load are the stress intensity factor, K, and the crack extension force or strain energy release rate, $\mathcal{G}$. The first emerges from the stress distribution near the tip of an infinitely sharp crack in a linear elastic material, given as [4,5]:

$$\sigma_x = \frac{K_I}{\sqrt{2\pi r}} f_1(\theta)$$

$$\sigma_y = \frac{K_I}{\sqrt{2\pi r}} f_2(\theta)$$

$$\sigma_{xy} = \frac{K_I}{\sqrt{2\pi r}} f_3(\theta)$$

where r and θ are polar co-ordinates at the crack tip. The only parameter affected by applied load is the stress intensity factor, K_I, which is in general a function of crack length and geometry as well as applied load.

The crack extension force, $\mathcal{G}$, was developed by Irwin from an energy point of view and can be regarded as a pseudo-force, brought on by applied load, acting to advance the crack tip. While both $\mathcal{G}$ and K were originally developed for the linear elastic case, the two are applicable under assumptions of nearly elastic behavior (i.e., the region of highly stressed yielded material is confined to a small enclave at the crack tip, called the plastic zone, by the surrounding elastic stress field). When this

assumption of "small scale yielding" can be made, $\mathcal{G}$ and K are simply related:

$$\mathcal{G}_I = \frac{(1 - \nu^2)}{E} K_I^2 \qquad \text{(plane strain)} \qquad (1)$$

where ν is Poisson's ratio and the subscript I applies to the opening crack extension mode which will henceforth be the only mode referred to. K and $\mathcal{G}$ completely describe the stress field surrounding the plastic zone at the crack tip. Their values at which fast fracture occurs are termed K_{Ic} and $\mathcal{G}_{Ic}$ (for plane strain) and are considered to be material constants. The reader is invited to read the more rigorous reviews of these concepts in the reference [6].

Stress corrosion crack growth and fatigue crack growth are common occurrences in both metals and polymers. Since they involve a slow, stable separation within the plastic zone, the behavior of a crack subjected to these processes can be characterized by K or $\mathcal{G}$. Most work in fatigue crack propagation has been done in metals and K rather than $\mathcal{G}$ has been explicitly used in nearly all the current models of fatigue crack propagation. The present investigation will show that it may be convenient to use $\mathcal{G}$ as well as K.

Prediction of Fatigue Crack Growth Behavior

A prediction of the fatigue crack propagation behavior in a service structure can be made if (1) the K or $\mathcal{G}$ history is known for the particular loading sequence, crack length, and geometry, and (2) the crack growth rate as a function of $\mathcal{G}$ or K history has been established from controlled tests on laboratory specimens.

Calculating K or $\mathcal{G}$ for particular geometries is a task for analysis by elasticity theory using analytical or numerical methods [7], or may

be done experimentally using the energy treatment of fracture. Trantina [8, 9] and Lin [10] used a finite element analysis to find K and $\mathcal{G}$ for cracks in an adhesive layer. Many analytical developments dealing with cracks in multi-layered elastic systems are given [11, 12] which obtain a great deal of generality with respect to the dimensions of the system. Ripling and Mostovoy [13] and Jemian and Ventrice [14] use experimental compliance measurements to obtain $\mathcal{G}$ in adhesive joints, although their values are restricted to the specific specimen and loading geometries. More recently, optical interference methods have been used to obtain K values from crack face displacements [15] in transparent polymer systems.

The dependence of crack growth rates upon K or $\mathcal{G}$ is established by using simple cracked specimens for which these loading parameters are well known. Testing involves introducing controlled K or $\mathcal{G}$ histories in the specimen and observing the ensuing crack growth rates. Modeling a crack tip that lies within an adhesive layer (IB) can thusly be accomplished with a monolithic specimen of the adhesive material. Care must be taken to ensure that the monolithic specimen and the adhesive layer are, in fact, the same material (i.e., identical composition and curing cycle) and that the effect of thermal residual stresses incurred during bonding are accounted for.

General Fatigue Behavior; Analytic Models

Paris, et al [16, 17], first suggested that for fatigue crack propagation in metals, the crack growth rate was almost exclusively dependent upon the change in stress intensity factor (ΔK) and only secondarily dependent on mean stress intensity and frequency. He proposed the following equation to describe the crack growth rate:

$$\frac{da}{dN} = (A)\ \Delta K^{n} \tag{2}$$

where A and n are constants. Paris cites several investigations into this phenomenon which support the validity of this empirical expression. Subsequently, many models were constructed that attempted to account for the effect of additional loading parameters (in terms of fracture mechanics variables) on the fatigue crack growth rate (see summaries by Plumbridge [18] and Pelloux [19]). Nearly all of these analytical models start from a metals viewpoint and deal with plastic deformation and slip at the crack tip. Uncomfortable discrepancies have arisen between the predicted and measured values of n in eq.(2) and as yet no one model is universally accepted.

Semi-Empirical Models; The Effect of Mean Stress Intensity

In the absence of any definitive analytical model, many researchers correlated the crack growth behavior to semi-empirical models that provided good fits to the observed data. The rate eq.(2) was modified to include the effects of mean stress intensity, R, as well as ΔK. This can be done by characterizing the constant amplitude loading spectrum by any two of the following parameters:

$$K_{min},\ K_{max},\ \Delta K,\ K_{mean},\ R = K_{min}/K_{max}$$

where all stress intensity factors are understood to be opening mode (the sliding mode, II, and tearing mode, III, not been used in experimental studies). One popular approach used by Foreman, et al [20], Hartman and Schijve [21], and Pearson [22] is to expand the relation proposed by Paris (2) to:

$$\frac{da}{dN} = \frac{A(\Delta K)^{n}}{[(1-R)K_{c}-\Delta K]^{p}} \tag{3}$$

where p is 1 or 1/2 for plane stress or plane strain, respectively, and n and A are fitted constants. This expression provides a very good description of aluminum growth rate data. Kitagawa [23] has shown this equation to hold also in PMMA.

An approach used by Arad, Radon, and Culver [24, 25] for polymers is shown to provide a convenient empirical description for PMMA, polycarbonate, and Nylon 6.6. The growth rate is given as:

$$\frac{da}{dN} = B\lambda^m \tag{4}$$

$$\lambda = K_{max}^2 - K_{min}^2 = 2\Delta K\, K_{mean} \tag{5}$$

where m is typically 1.8 to 3.0.

Other variables to be considered as affecting the growth rate are loading rate (frequency), temperature, and humidity (environment). It is expected and has been shown [26] that energy absorbing viscous mechanisms in polymers cause rate effects in fatigue crack growth (although present data on epoxy is inconclusive). It is therefore necessary to monitor frequency or strain rate when extracting growth rate data from polymers.

APPARATUS AND TESTING

Specimens

The tapered-double-cantilever-beam (TDCB) specimen shown in Fig. 2 was chosen to extract baseline crack growth rate data. Ripling and Mostovoy [27] have used this specimen to measure growth rates in an epoxy layer constrained by aluminum adherends. Marshall, et al [28, 29], have used it to extract stress corrosion cracking and fatigue growth rate data in various polymers with excellent results. Srawley and Gross [30] have provided a stress analysis of this specimen using the boundary collocation technique and Ripling and Mostovoy have analyzed the specimen from an energy point of view using the strain energy release rate, $\mathcal{G}$.

The TDCB is very compliant so that it can be easily pre-cracked to produce a sharp, natural starting crack. As shown in the appendix, K or $\mathcal{G}$ is independent of crack length in this specimen geometry and depends only upon applied load. Also, an initially uneven crack front stays nearly the same shape, all points growing at the same rate (in the plate specimens an eccentric crack front becomes more eccentric under fatigue). For these and other reasons, the TDCB was found more desirable to work with than the plate specimens commonly used to study fatigue crack growth rates.

Since the stress state near (but removed from) the crack tip is highly biaxial, which is unique to beam type specimens, the crack is not directionally stable and sidegrooves were necessary to constrain the crack growth direction. Rectangular notches (0.006 in. wide by 0.090 in. deep) were found satisfactory. The V-notch sidegroove, popular in metallic TDCB work, was not suitable for these epoxy specimens.

Plates of 0.40 inch thickness were cast of 15 parts-per-hundred tetraethylene-pentamine (TEPA) hardener in DER 332* epoxy resin at 150°F for

*Tradename of the Dow Chemical Company

4 hours. These were postcured at 320°F for 4 hours with a rise and cool rate of 10°F/hr. to prevent thermal stresses and checked in a polariscope. Specimens were then machined from the plates in configurations shown in Figs. 2 and 5.

Testing

All crack growth specimens were loaded in an Instron fatigue machine at a constant crosshead rate between load limits. Loading frequency (or strain rate) varied only slightly. Crack growth rates were determined from TDCB specimens using the following scheme. The specimen was cycled between constant load limits (ΔK constant) for several thousand cycles and crack tip advance ($\underline{\Delta a}$, as measured by a spotting scope) noted. After several such runs, each at a different value of ΔK, the specimen was broken and bands of differing surface roughness each representing one value of $\underline{\Delta a}$ for each ΔK could be examined under a microscope to determine a more precise value of $\underline{\Delta a}$. The growth rate (da/dN) was taken as $\Delta a/\Delta N$. In this manner, several data points could be determined from one TDCB specimen.

Most of the tests were conducted at room temperature, and humidity was noted to be stable (35%$\pm$5% R.H.). It is possible for an epoxy to stress corrosion crack under these conditions so constant load tests were conducted on the TDCB specimens. It was found that the static stress corrosion crack growth rate was quite negligible compared to the fatigue growth rate.

RESULTS AND DISCUSSION

TDCB Fatigue Crack Growth Rates

The most commonly used representation for fatigue crack growth data is the graph of da/dN versus ΔK with different data lines for various values of the stress intensity ratio, R. This graph of the TDCB epoxy data is shown in Fig. 3. It should be noted that the slopes for the different R values are the same with only the intercept as variable, within experimental error. By changing the value of R from R = 0.1 to R = 0.7, the growth rate is changed nearly two orders of magnitude which reflects a great dependence on mean stress intensity.

In selecting an empirical formula to account for this dependence it was most satisfying to modify the model developed for several other polymers by Arad, Radon, and Culver [24,25]. They postulated the growth rate as dependent upon the parameter λ, where:

$$\lambda = K_{max}^2 - K_{min}^2 = 2\Delta K (K_{mean}) \tag{6}$$

and

$$\frac{da}{dN} = A(\lambda)^m \tag{7}$$

Since $\mathcal{G}$ is proportional to K^2, a similar expression may be proposed in terms of $\Delta\mathcal{G}$:

$$2\Delta K\ (K_{mean}) = K_{max}^2 - K_{min}^2 = \frac{E}{(1-\nu^2)}\,\Delta\mathcal{G} \tag{8}$$

$$\frac{da}{dN} = B(\Delta\mathcal{G})^m \tag{9}$$

The crack growth rate data from the epoxy TDCB specimens shown in Fig. 4 verifies that this expression provides a good fit to the data. This straight line fit produces the following relationship:

$$\frac{da}{dN} = 5.9(10^{-5})\ \Delta\mathcal{J}^{5.5} \qquad (10)$$

It may well be that the linear log-log relation is presumptuous particularly since such data in other polymers is only roughly linear. Mostovoy and Ripling [31] choose to fit parabolic-shaped curves to similar data for epoxies and researchers in metals often fit quite irregular curves to such data, especially when the element of stress corrosion is involved. Also, after a close look at the data points on Fig. 4 one might even be led to conclude that there are in fact three different fitted lines for the three different values of R with slightly different intercept, B, and/or slope, $\underline{m}$, values. However, in view of the scatter band encountered in the present fatigue growth data and that an order of magnitude life estimate is often all that is required in a design situation, the simple relationship of eq.(5) is sufficient to describe the trends in fatigue crack growth behavior in this epoxy over this wide range of growth rates.

The high value of the exponent $\underline{m}(5.5)$ in relation to other polymers (1.8 to 3.0, [24, 25]) indicates a higher dependence of the crack growth rate upon $\Delta\mathcal{J}$ or $\underline{\lambda}$ in epoxy. When compared with exponents $\underline{n}$ in theories involving ΔK^n, the value $\underline{n} = 10$ for epoxy (Fig. 3) is much higher than for metals where $\underline{n}$ is typically 2.0 to 5.0.

Although still empirical in nature, the expression (9) provides an appealingly simple manner in which to express fatigue crack growth rates for these polymeric materials. The fatigue crack growth rate equation has been reduced from one containing two loading parameters (e.g., K_2 and K_1, ΔK and R, etc.) to one containing only one loading parameter ($\Delta\mathcal{J}$). That the simple substitution of $\Delta\mathcal{J}$ for ΔK in the original form developed by Paris for metals (eq.(2)) accounts for the effect of R as well as ΔK

is at first puzzling. It must be noted, however, that this can only be accomplished when the growth rate can be described by the particular model proposed by Arad, et al. Specifically, the growth rate must be proportional to the $\underline{m}$ power of K_{mean} and also proportional to the $\underline{m}$ power of ΔK_I which yields eq.(7). This appears to be the case in the present epoxy as well as the three polymers cited above. Since Kitagawa [23] has fitted the model of Forman also to PMMA, it may be that the two models are not substantially different in practice.

Barsom [36] has suggested the use of $\Delta\mathcal{J}$ as the principle variable in metals noting that the growth rates may be normalized for many metals by considering $K_I/\sqrt{E}$ as the loading variable. The analysis is restricted in that only zero-to-maximum tensile loading (R=0) is considered, but a good empirical fit for high strength aluminum and titanium alloys was provided by the expression:

$$\frac{da}{dN} = D(\Delta\mathcal{J})^{1.0}$$

The use of $\Delta\mathcal{J}$ as the principle variable easily lends itself to an interpretation of fatigue crack growth in terms of crack opening displacement (COD) since:

$$\mathcal{J} = \delta\ \sigma_y$$

where $\underline{\delta}$ is the total crack opening displacement and $\underline{\sigma_y}$ the yield strength.

Using $\Delta\mathcal{J}$ as the principle variable in the crack growth rate eq.(9) offers promise in its simplicity and lends itself easily to a possible energy or COD interpretation of the fatigue crack growth process in polymers.

Plate Specimen Data

To collaborate the data taken from the TDCB specimens, tests were made on center-crack plate (CCP) specimens for which K_I may be accurately calculated when crack length and nominal stress are known. Center-crack plates were precracked by wedging a small sawcut, then loading between constant load limits and monitoring the crack growth. Difficulty was encountered in that the crack front became somewhat eccentric making the latter crack length measurements difficult. This problem seems to be encountered often in the testing of polymer CCP specimens and points up an advantage to using the TDCB geometry.

When cycled between constant load limits, the crack length history is that shown in Fig. 5. The results of reducing this crack length versus cycles to growth rate (da/dN) versus ΔK is given in Fig. 6. The data points lie within the scatter band of the TDCB data.

Elevated Temperature Tests

Tests were performed on a TDCB at an elevated temperature (200°F) with R equal to 0.1 and the results shown in Fig. 7. The net effect of this increase in temperature is to increase the growth rate. A small decrease in the slope, from $\underline{n} = 10$ to $\underline{n} = 6$, is indicated, also.

Surface Morphology and Growth Mechanism

The mechanism for fatigue crack propagation in non-crystalline highly-crosslinked thermoset resins such as epoxy is not well understood. These materials can be described as being highly resistant to flow mechanisms and therefore quite brittle. Figure 1 displays a tensile loading cycle from a cylindrical specimen of the present epoxy. The cyclic curve was virtually independent of strain rate over several orders of magnitude

(0.002 to 2.0/min.). There was no observable permanent plastic strain but the hysterisis indicates the presence of a viscous mechanism. These materials are also considered to be non-linear in the elastic sense.

Photomicrographs of the fatigue fracture surface reveal no observable fatigue striations but show a rough surface hackle whose features are roughly one to two orders of magnitude larger than the average growth per cycle. There is actually no justification to assume that crack propagation is continuous on the microscale, although it appears to be so on the macroscale (0.01 in. for da/dN = 0.0001). Figures 7-14 show the fatigue fracture surface with dimensions as noted. In each figure the crack growth direction is indicated by the arrow.

It is enlightening to look at the work done in describing fatigue crack propagation in metals. While in the ductile pure metals, fatigue crack growth is almost totally ductile striation formation arising from successive blunting and re-sharpening of the crack tip, several researchers (McClintock [32], Laird [33], and Frost [34]) note that in high strength aluminum alloys, for example, two mechanisms appear to be present. The first is the ductile striation formation; the second, a stable micro-crack propagation ahead of the main crack. McClintock and others attribute the latter to cleavage fracture at inclusion sites near the crack tip. Pelloux [35] presents evidence that although microscale measurements of striation spacing predict the growth rate in these aluminums as given from plasticity models where $\underline{n} = 2$ (see references [18, 19]), this cleavage mechanism makes the observed growth rate much higher. Frost [34] attributes the dependence on K_{mean} to this cleavage mechanism in discussing high strength aluminum alloys. Laird [33] describes how such a combined ductile-cleavage mechanism might occur and McEvily, et al [1], describe a similar possible

mechanism for polymers. Although cleavage is associated with crystallographic planes in metals, a cleavage-like or branch cracking mechanism in epoxy could explain the finger markings on the epoxy fatigue fracture surfaces (Figs. 8-14). These markings are similar to the "river markings" running parallel to the crack propagation direction that are typically observed as a result of cleavage-assisted fatigue crack propagation in the above metals. Tomkins and Briggs [2] suggest that fatigue crack propagation in epoxy smooth specimen fatigue consists of this slow, stable cleavage-like or branch cracking mechanism. Any branch cracks that did not result in fracture as the crack tip passed would be very difficult to see on an epoxy fatigue surface since they would close due to the low ductility of the material.

The epoxy polymers may well be a prime example of a material where this cleavage-like or branch cracking mechanism is dominant. They have very little ductility, show no well defined fatigue striations, exhibit a fracture surface similar to the river markings referred to by Laird (above), have a growth rate highly dependent upon K_{mean}, and yield very high values for the exponent $\underline{m}$ in eq.(9).

SUMMARY

This investigation has used the tapered-double-cantilever-beam (TDCB) specimen to determine fatigue crack growth rates in a representative epoxy resin polymer. The motivation for this study came from the widespread use of this type of polymer as an adhesive in adhesively-joined systems where quantitative prediction of the fatigue performance is essential. These results taken together with the observed behavior of similar polymers should lead to practical design criteria for the tolerance of flaw growth in these polymeric materials. The results may be summarized as follows:

1. The epoxy system investigated (DER 332-TEPA, cured as described) exhibits regular fatigue crack propagation in ambient and high temperature environments that appears to be continuous on the macroscale. The TDCB specimen with side grooves worked very well in determining the growth rates.

2. A semi-empirical model for the fatigue crack propagation is proposed based on the change in strain energy release rate or crack extension force, $\Delta\mathcal{J}$, that inherently accounts for the effect of mean stress intensity in this epoxy as well as other polymers. This relation which provides a fit to the data for epoxy is:

$$\frac{da}{dN} = 5.9(10^{-5})\ \Delta\mathcal{J}^{5.5}$$

3. Micrographs of the fracture surface show no observable fatigue striations but indicate the presence of some cleavage-like or branch cracking mechanism of a type described by several other authors.

LIST OF REFERENCES

1. A. J. McEvily, R. C. Boethner, and T. L. Johnston, "On the Formation and Growth of Fatigue Cracks in Polymers," Fatigue: An Interdisciplinary Approach, ed. Burke, Reed, and Weiss, Syracuse University Press, (1963), p. 95.

2. B. Tomkins and W. D. Briggs, "Low Endurance Fatigue in Metals and Polymers: Parts I, II, and III," J. Materials Science, v. 4, p. 532.

3. C. E. Feltner, "On the Mechanical Behavior and Fracture Morphology of Epoxy Resin," Dept. of T.&A.M. Report No. 224, U. of Ill. at Urbana (1962).

4. H. M. Westergaard, "Bearing Pressures and Cracks," Trans. ASME, J. of Applied Mechanics (June 1939), p. A-49.

5. G. R. Irwin, "Analysis of Stresses and Strains Near the End of a Crack," Trans. ASME, J. of Applied Mechanics, v. 24 (1957), p. 361.

6. Fracture Toughness Testing, American Society for Testing and Materials, (1964), ASTM STP 381.

7. G. C. Sih, ed., Mechanics of Fracture 1; Methods of Analysis and Solutions of Crack Problems, Noordhoff International Publishers, Leyden, The Netherlands (1973).

8. G. G. Trantina, "Fracture Mechanics Approach to Adhesive Joints," Dept. of T.&A.M. Report No. 350, U. of Ill. at Urbana (August, 1971).

9. G. G. Trantina, "Combined Mode Extension in Adhesive Joints," Dept. of T.&A.M. Report No. 352, U. of Ill. at Urbana (November, 1971).

10. Fong-tsu Lin, "The Elastic Stress Analysis of a Bi-Material Plate with a Crack Normal to the Interface," Dept. of T.&A.M. Report No. 356, U. of Ill. at Urbana (May, 1972).

11. F. Erdogan and G. Gupta, "The Stress Analysis of Multi-Layered Composites with a Flaw," International J. of Solids and Structures, v. 7 (1971), p. 39.

12. G. C. Sih and P. D. Hilton, "A Laminate Composite with a Crack Normal to the Interface," International J. of Solids and Structures, v. 7 (1971), p. 913.

13. S. Mostovoy and E. Ripling, "Interphase Fracturing of Composite Bodies," Materials Research Lab., Inc., Glenwood, Illinois (June, 1967).

14. W. A. Jemian and M. B. Ventrice, "The Fracture Toughness of Adhesive Bonded Joints," J. of Adhesion, v. 1 (July, 1966), p. 190.

15. P. B. Crosley, S. Mostovoy, and E. J. Ripling, "An Optical-Interference Method for Experimental Stress Analysis of Cracked Structures," Engineering Fracture Mechanics, v. 3 (1971), p. 421.

16. P. C. Paris and H. H. Johnson, "Sub-Critical Flaw Growth," Engineering Fracture Mechanics, v. 1, no. 1 (June, 1968), p. 3.

17. P. C. Paris, "The Fracture Approach to Fatigue," Fatigue, an Interdisciplinary Approach, Proc. of the Tenth Sangamore Army Materials Research Conference, Syracuse University Press (1964), p. 107.

18. W. J. Plumbridge, "Review: Fatigue Crack Propagation in Metallic and Polymeric Materials," J. Materials Science, v. 7 (1972), p. 939.

19. R. Pelloux, "Review of Theories and Laws of Fatigue Crack Propagation," Proc. Air Force Conf. on Fatigue and Fracture of Aircraft Structures and Materials, Miami Beach (December, 1969), p. 409.

20. R. G. Foreman, V. E. Kearney, and R. M. Engle, "Numerical Analysis of Crack Propagation in Cyclic-Loaded Structures," J. of Basic Engineering, v. 89 (1967), p. 459.

21. A. Hartman and J. Schijve, "The Effects of Environment and Load Frequency on the Crack Propagation Law for Macro-Fatigue Crack Growth and Aluminum Alloys," National Aeronautical Research Institute, Amsterdam, to be published.

22. S. Pearson, "Effect of Mean Stress on Fatigue Crack Propagation in Polymeric Materials," Engineering Fracture Mechanics, v. 1 (1972), p. 9.

23. M. Kitagawa, "The Effect of Stress Ratio on the Fatigue Crack Growth in High Polymers," J. of the Soc. of Materials Science, Japan, v. 21 (1972), p. 859.

24. S. Arad, J. C. Radon, and L. E. Culver, "Fatigue Crack Propagation in PMMA; The Effect of the Mean Value of Stress Intensity Factor," J. of Mechanical Engineering Science, v. 13, p. 75.

25. S. Arad, J. C. Radon, and L. E. Culver, "Design Against Fatigue Failure in Thermoplastics," Engineering J. of Fracture Mechanics, v. 4 (1972).

26. J. A. Manson, R. W. Hertzberg, and H. Nordberg, "Fatigue Crack Propagation in Polymeric Materials," J. of Materials Science, v. 5 (1970), p. 521.

27. S. Mostovoy, P. Crosley, and E. Ripling, "Use of Crack-line Loaded Specimens for Measuring Plane Strain Fracture Toughness," Materials Research Lab., Inc., Glenwood, Illinois (1966).

28. G. P. Marshall, L. E. Culver, and J. G. Williams, "Crack and Craze Propagation in Polymers: A Fracture-Mechanics Approach," Plastics and Polymers (February, 1969), p. 75.

29. G. P. Marshall, L. E. Culver, and J. G. Williams, "Environmental Stress Crack Growth in Low-Density Polyethylenes," Plastics and Polymers (April, 1970), p. 95.

30. J. E. Srawley and B. Gross, "Stress Intensity Factors for Crackline-loaded Edge Crack Specimens," NASA Tech. Note TN D-3820.

31. S. Mostovoy and E. Ripling, "Fracturing Characteristics of Adhesive Joints," Final Report (January 30, 1972), Materials Research Lab., Glenwood, Ill.

32. F. A. McClintock, "On the Plasticity and Growth of Fatigue Cracks," Fracture of Solids, ed. Drucker and Gilman, Gorden and Breach Science Publishers, New York (1963), p. 65.

33. C. Laird, "The Influence of Metallurgical Structure on the Mechanisms of Fatigue Crack Propagation," Fatigue Crack Propagation, American Society for Testing and Materials, ASTM-STP 415 (1967), p. 131.

34. N. E. Frost, "The Growth of Fatigue Cracks," Proc. First International Conference on Fracture, Sandai, Japan, p. 1433.

35. R. Pelloux, "Fractographic Analysis of the Influence of Constituent Particles on Fatigue Crack Propagation in Aluminum Alloys," Am. Soc. for Metal, v. 57 (1964), p. 511.

36. J. M. Barsom, "The Dependence of Fatigue Crack Propagation on Strain Energy Release Rate and COD," Damage Tolerance in Aircraft Structures, ASTM-STP 486 (1971), p. 1.

APPENDIX

Analysis of TDCB Specimen

In general, for a body under point loading:

$$\mathcal{G} = \frac{1}{2} P^2 \frac{\partial C}{\partial A}$$

where

C = specimen compliance defined as the inverse of the stiffness (for linear elastic materials)

A = area of crack surface (one surface only)

For the TDCB specimen, this expression can be expanded [17] to:

$$\mathcal{G} = P^2 \gamma$$

Where γ is a geometric variable dependent upon the contour of the specimen and crack length. Using straight sloped sides the value of γ is very nearly constant with respect to crack length when the crack tip lies in an area near the center of the specimen. Thusly:

$$\mathcal{G} \propto P^2$$

in this area. Also, from the theory of linear elasticity:

$$\mathcal{G}_I = \frac{(1-\nu^2)}{E} K_I^2$$

$$K_I \propto P$$

The area of specimen validity and γ were determined from a compliance calibration (Fig. 2) from which:

$$\frac{\partial C}{\partial A} = \frac{1}{b_n} \frac{\partial C}{\partial a} = \frac{1}{b_n} \; 8.0 \; (10^{-4})$$

where b_n is the width of the fracture surface. K_I and $\mathcal{G}_I$ were subsequently calculated for each specimen.

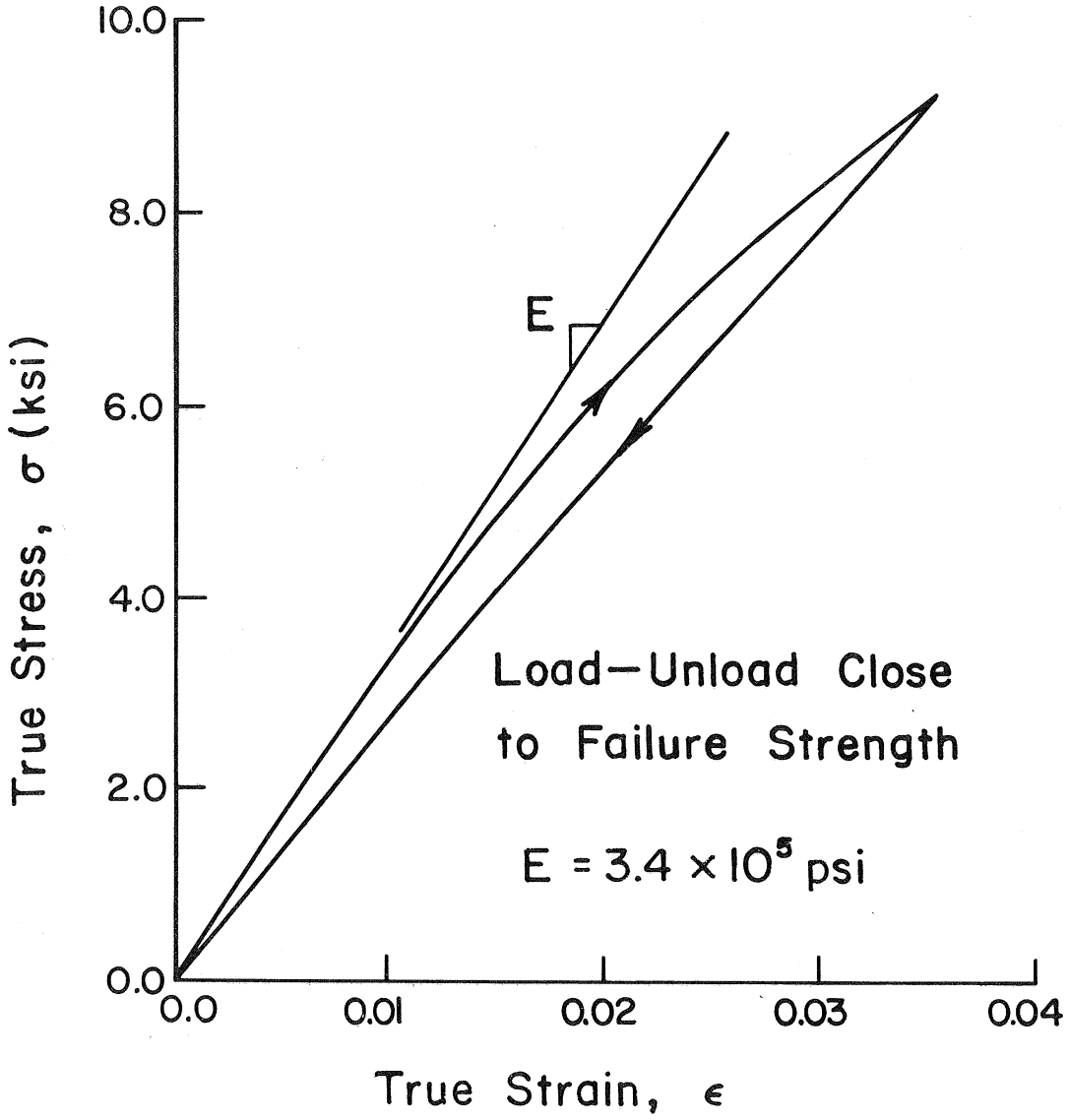

FIG. 1 Tensile Stress–Strain Curve of the Epoxy Polymer

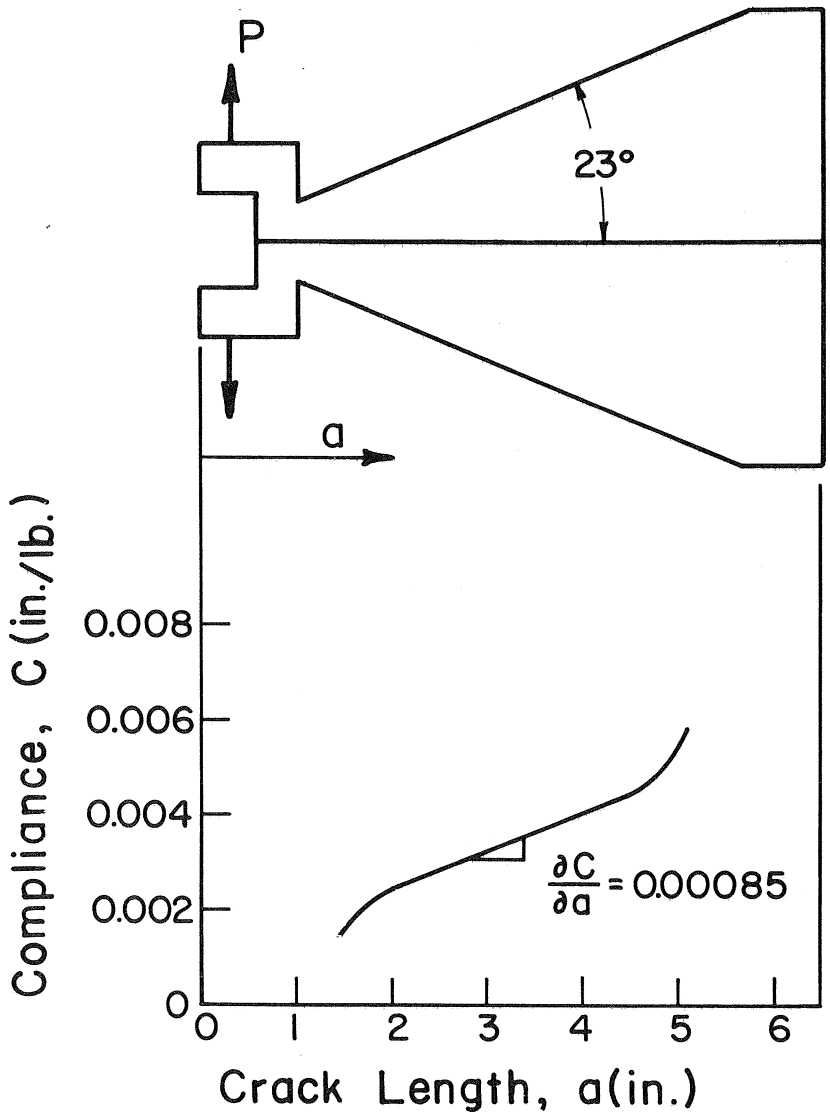

Fig. 2 TDCB Specimen with Compliance Curve

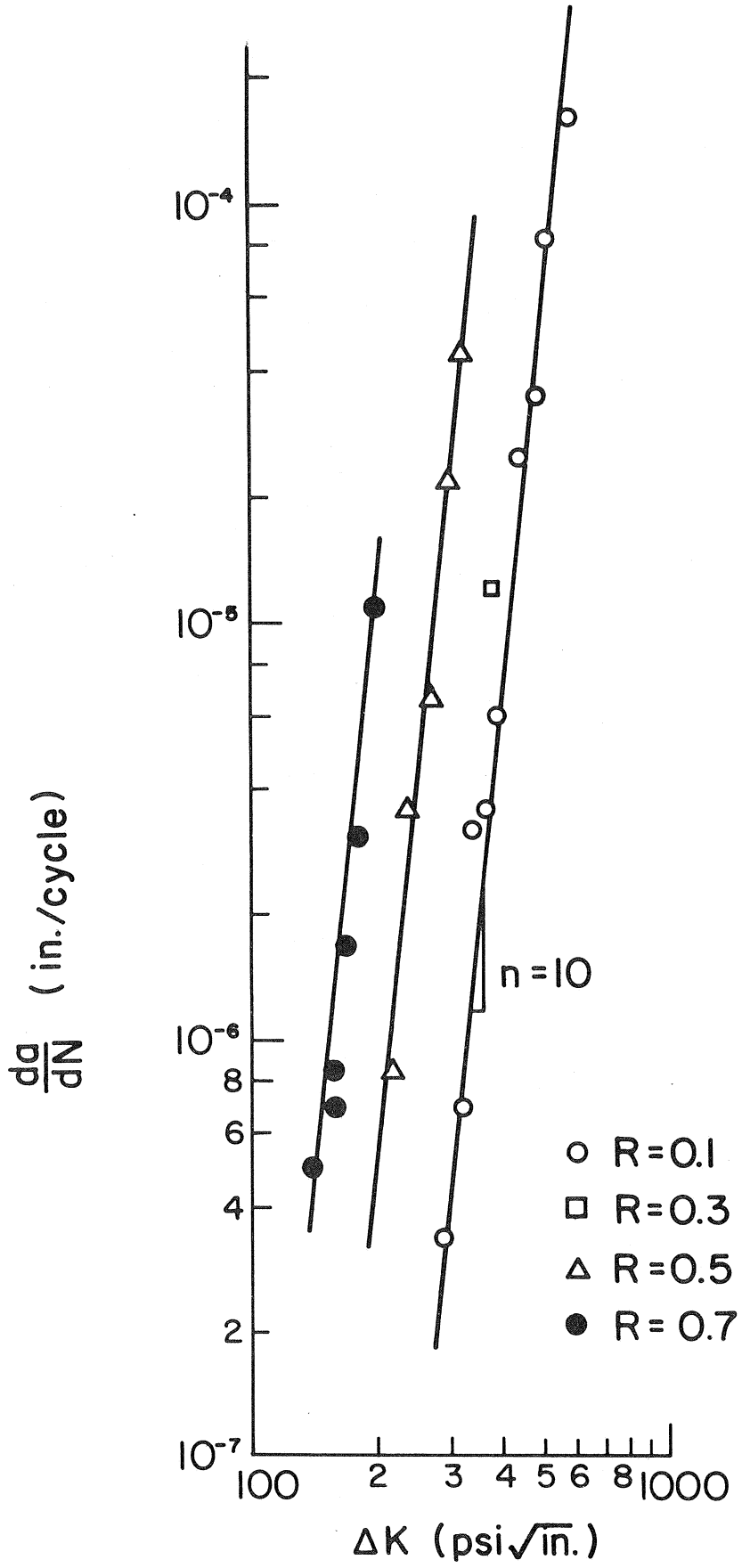

Fig. 3 Fatigue Crack Growth Rate as a Function of ΔK and R from Epoxy TDCB Specimen

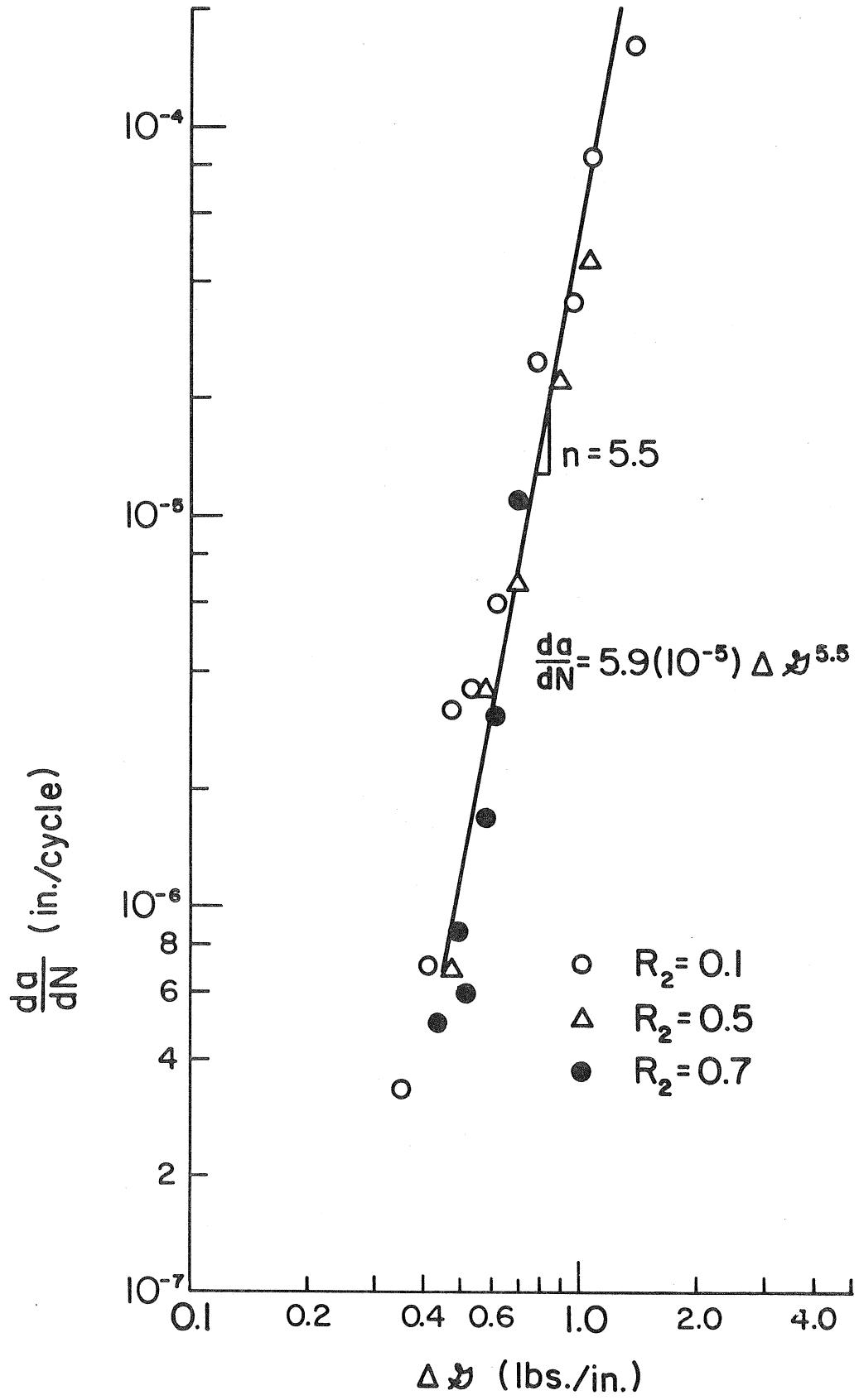

Fig. 4 Fatigue Crack Growth Rate as a Function of $\Delta\mathcal{D}$ from Epoxy TDCB Specimen

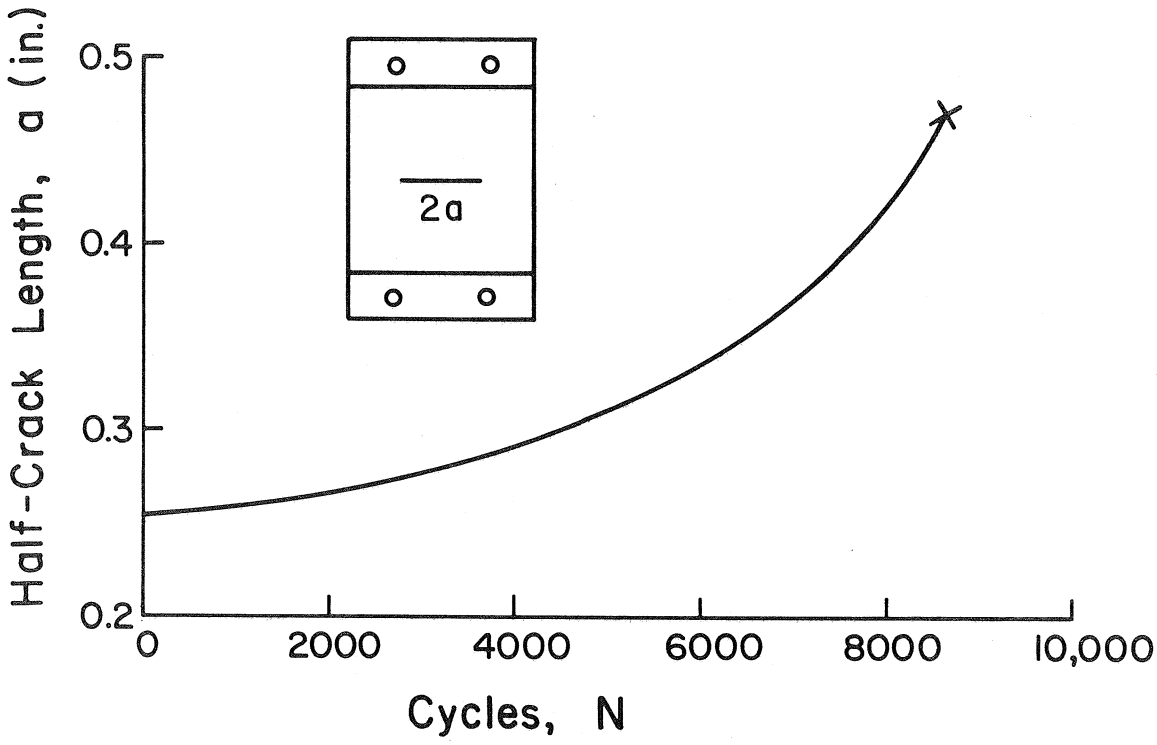

Fig. 5 Crack Growth History in the Epoxy Center Crack Plate

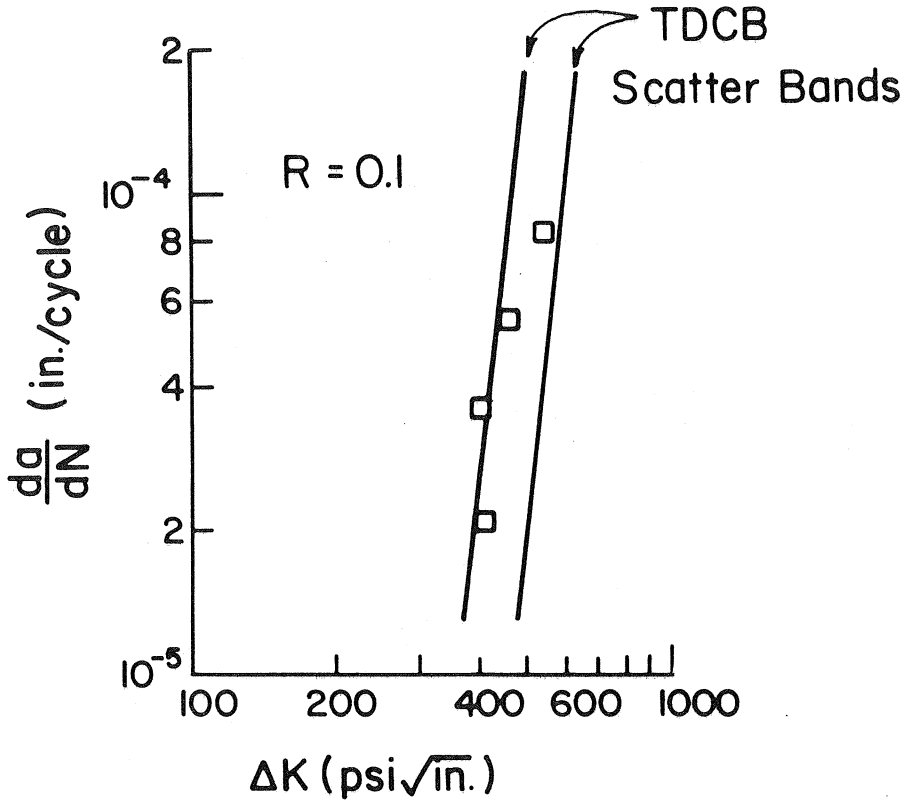

Fig. 6 Comparison of Fatigue Crack Growth Rates in Center Crack Plate and TDCB Specimen

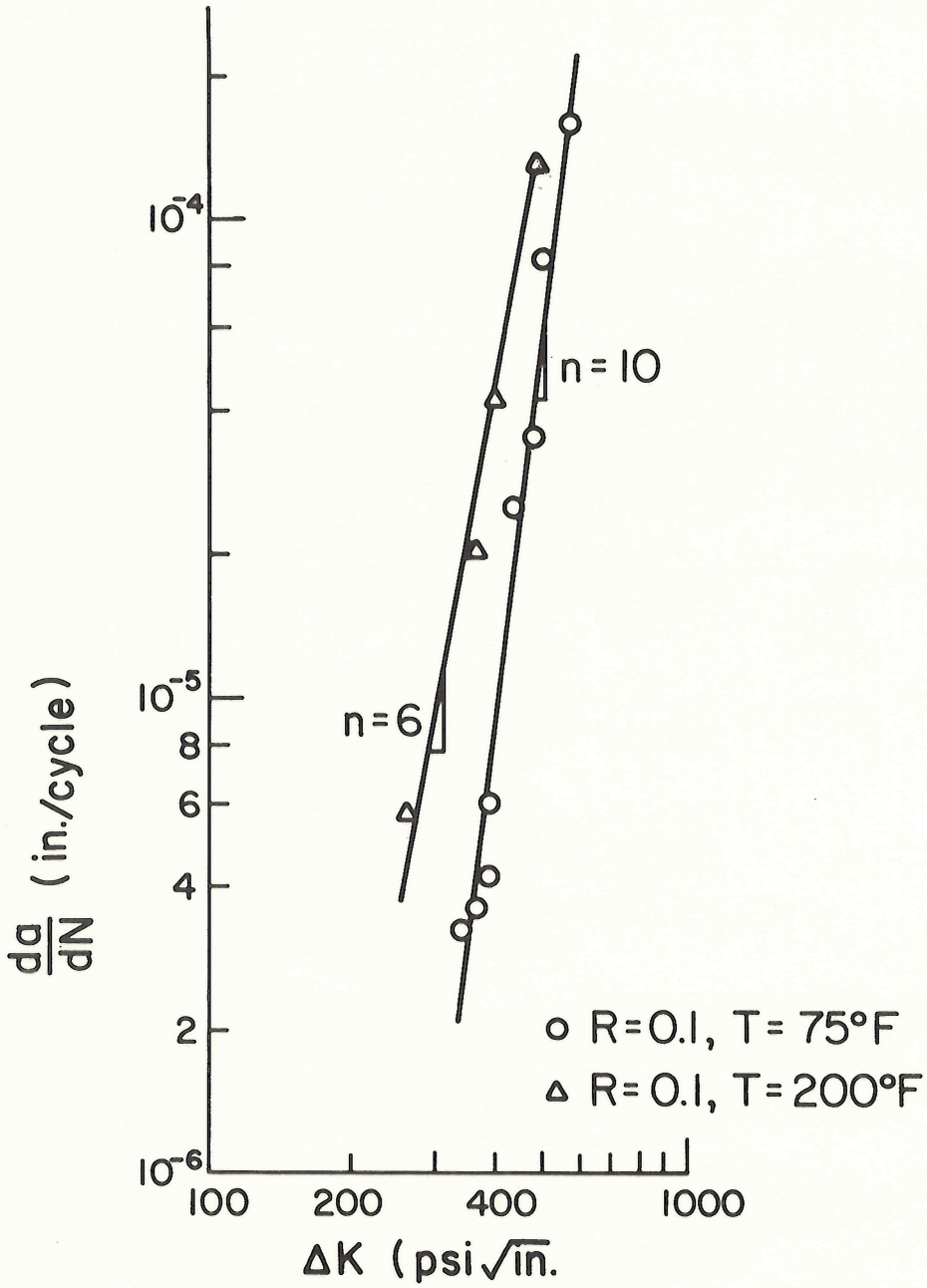

Fig. 7 Comparison of Fatigue Crack Growth Rates at Ambient and Elevated Temperatures

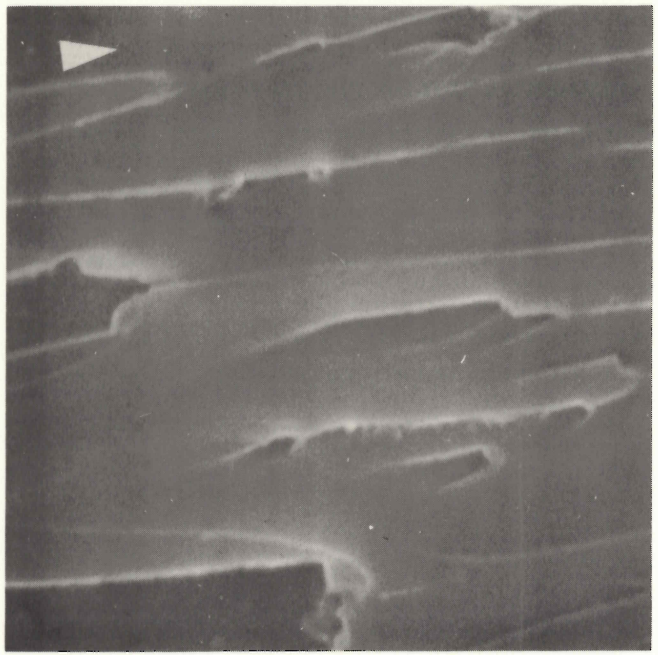

$\frac{da}{dN} = 9(10^{-5})$ $\quad \Delta N = 12$ (0.001)

1500×

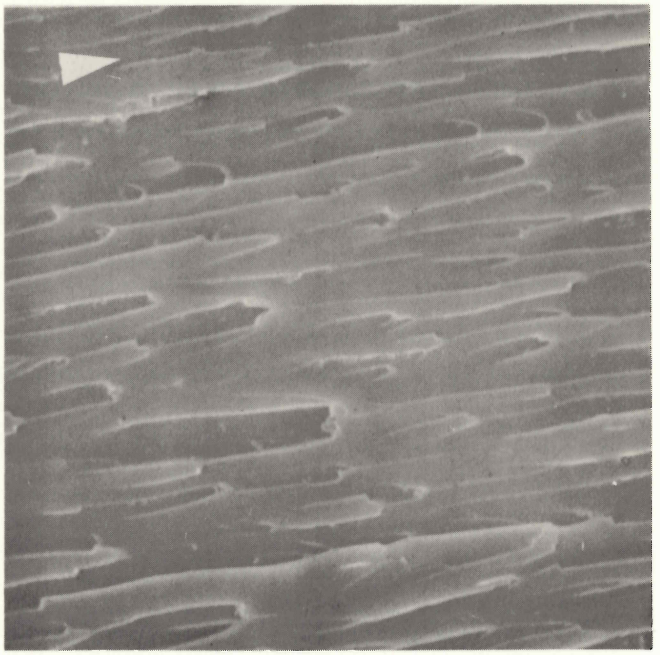

$\frac{da}{dN} = 9(10^{-5})$ $\quad \Delta N = 36$ (0.003)

500×

Figs. 8 & 9 Fatigue Fracture Surfaces

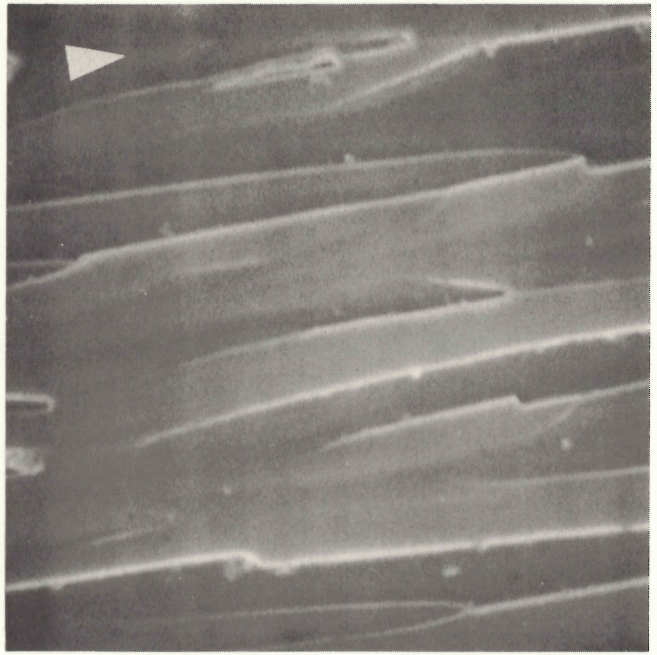

$\frac{da}{dN} = 4(10^{-5})$ $\longleftarrow \frac{\Delta N = 30}{0.001} \longrightarrow$

1500×

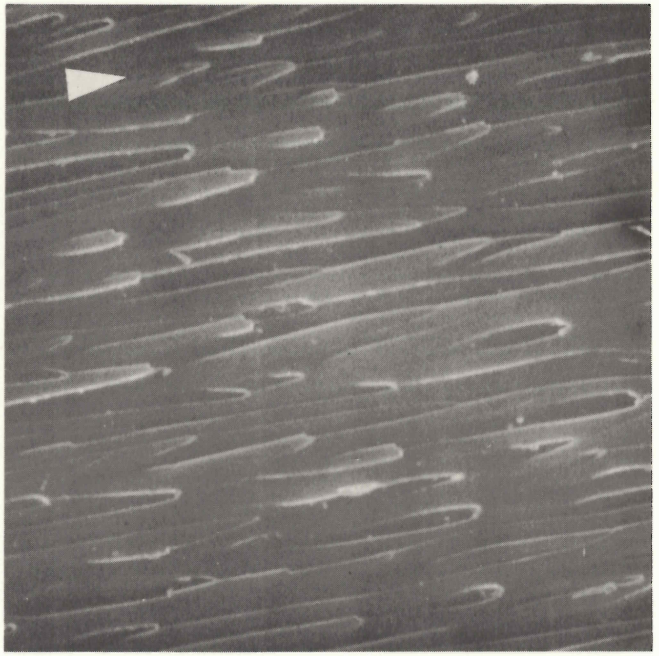

$\frac{da}{dN} = 4(10^{-5})$ $\longleftarrow \frac{\Delta N = 90}{0.003} \longrightarrow$

500×

Figs. 10 & 11 Fatigue Fracture Surfaces

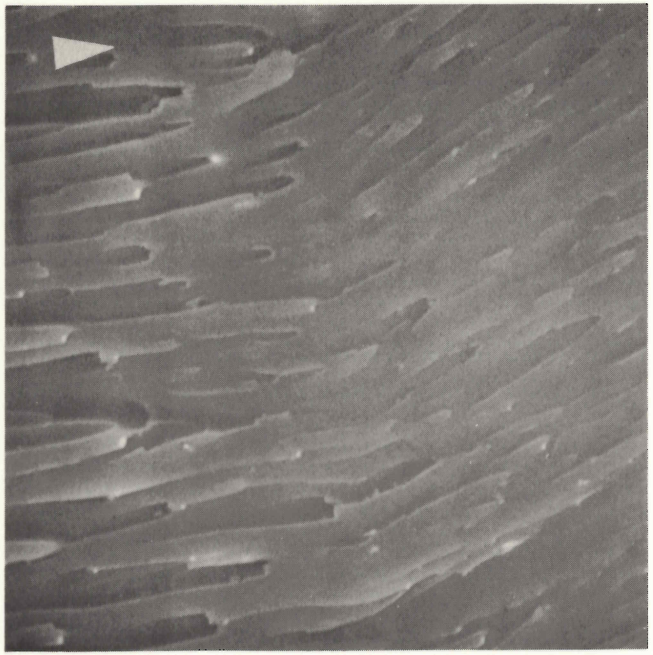

$\frac{da}{dN} = 10^{-4}$ $\quad \Delta N = 40$ (0.003)

500×

Fig. 12 Fatigue–Fast Fracture Transition

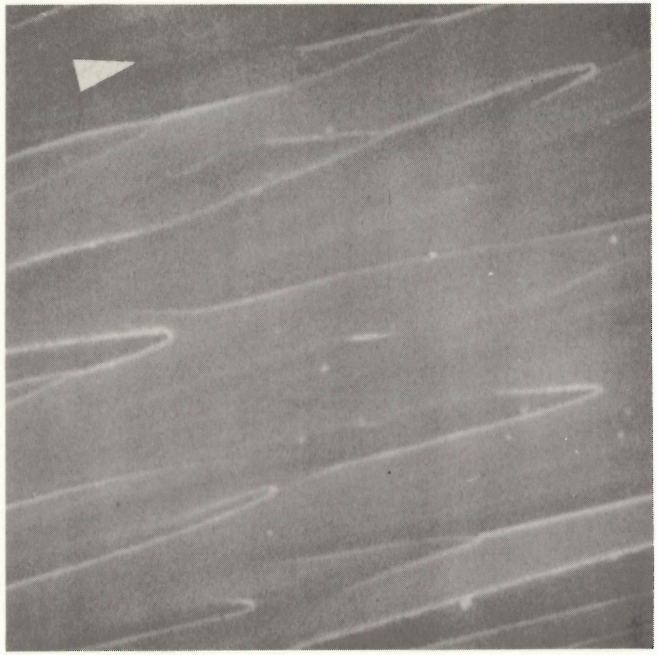

$\frac{da}{dN} = 10^{-4}$ $\quad \Delta N = 2000$ (0.0005)

2000×

Fig. 13 Fatigue Fracture Surface

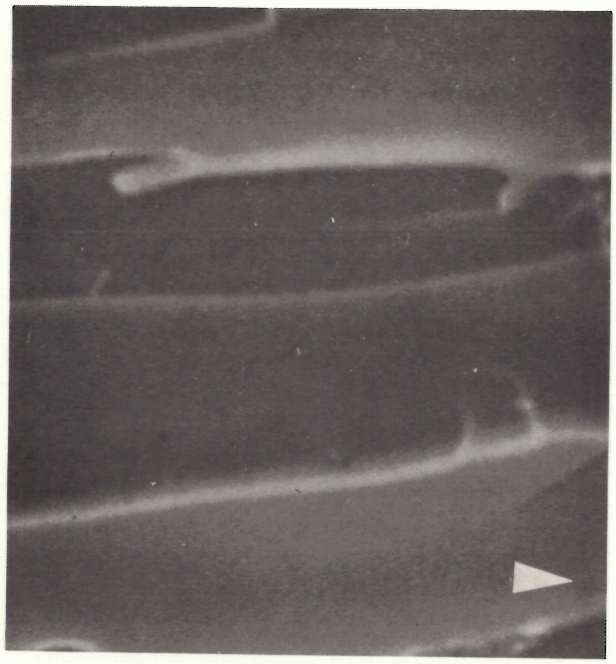

Fig. 14 Fatigue Fracture Surface at Resolution Limit